

# State-Periodic Adaptive Compensation of Cogging and Coulomb Friction in Permanent-Magnet Linear Motors

Hyo-Sung Ahn, *Student Member, IEEE*, YangQuan Chen, *Senior Member, IEEE*, and Huifang Dou, *Member, IEEE*

**Abstract**—This paper focuses on the state-periodic adaptive compensation of cogging and Coulomb friction for permanent-magnet linear motors (PMLMs) executing a task repeatedly. The cogging force is considered as a position-dependent disturbance and the Coulomb friction is non-Lipschitz at zero velocity. The key idea of our disturbance compensation method is to use past information for one trajectory period along the state axis to update the current adaptation law. The new method consists of three different steps: 1) in the first repetitive trajectory, an adaptive compensator is designed to guarantee the  $l_2$ -stability of the overall system; 2) from the second repetitive trajectory and onward, a trajectory-periodic adaptive compensator stabilizes the system; and 3) to make use of the stored past state-dependent cogging information, a search process is utilized for adapting the current cogging coefficient. We illustrate the validity of our state-periodic adaptive cogging and friction compensator by actual PMLM-model-based simulation.

**Index Terms**—Adaptive control, cogging force, Coulomb friction force, state-dependent disturbance, trajectory-periodic adaptation.

## I. INTRODUCTION

PERMANENT-MAGNET (PM) motors are the most popularly used electromechanical devices for accurate speed and position control of the linear system or rotary system. In parallel with the popularity of PM motors, the nonlinear torques inherent to PM motors have been addressed in numerous articles [1]–[3]. In particular, in [4], load torques, friction effects, and cogging torques are addressed as inherent torques of the PM stepper motors; and in [5] and [6], friction, cogging, and reluctance forces are modeled for iron-core permanent-magnet linear motors (PMLMs). As explained in [7], the cogging forces are due to the interaction between the permanent magnets and the steel teeth of the primary section; and the friction force is a velocity-dependent nonlinear disturbance that is inherent to most of the electromechanical systems.

In PMLMs, nonlinear mechanical disturbances such as backlash are greatly reduced, while the cogging forces are considered as the main disturbance [3], [5]. However, static friction force such as Coulomb friction is still a dominant disturbance

and should be compensated for accurate speed and position control of PMLMs. Thus, in this paper, we focus on the compensation for the disturbance of cogging force and the Coulomb friction. These disturbances are compensated by the trajectory-periodic adaptation based on Lyapunov stability analysis on the time axis.

Cogging forces are position-dependent periodic disturbances due to the slotted nature of the primary core [3], [6], and generally it is modeled as Fourier expansion [1], [2]. However, in control strategies, it has been modeled as a simple sinusoidal signal of the displacement signal  $x$  such as

$$F_{\text{cogging}} = A \sin(\omega x + \varphi) \quad (1)$$

and the unknown parameters such as  $A$ ,  $\omega$ , and  $\varphi$  have been compensated by a certain parameter adaptation scheme [4], [5], [8]. However, this approach does not represent high-order terms in the Fourier series; hence, it cannot compensate the cogging force completely. In this paper, we do not assume any model such as (1); instead, it is considered that the cogging force could be any kind of Fourier expansion such as

$$F_{\text{cogging}} = \sum_{i=1}^{\infty} A_i \sin(\omega_i x + \varphi_i) \quad (2)$$

where  $A_i$  is the amplitude,  $\omega_i$  is the state-dependent cogging force frequency, and  $\varphi_i$  is the phase angle. In order to compensate cogging force of (2), it is suggested to make use of the periodicity of cogging disturbance on the repetitive trajectory. Note that cogging force waveform is periodic over pole pitches in PMLMs [2].

In the control community, Coulomb friction force compensation has been studied widely in [9] and [10], and many efforts have been devoted in the late 1980s and early 1990s to compensate friction force [11]–[15]. After these early works, several adaptive friction compensation controllers have been suggested [16]–[19]. We can see that the friction compensation is still considered a hot topic.

In this paper, we focus on the state-periodic adaptive compensation of cogging and Coulomb friction for PMLMs executing a given task repeatedly. The cogging force is considered as a position-dependent disturbance and the considered Coulomb friction is non-Lipschitz at zero velocity. The key idea of our disturbance compensation method is to use one trajectory period past information along the state axis to update the current adaptation law. The new method consists of three different steps: 1) in the first repetitive trajectory, an adaptive compensator is designed

Manuscript received September 19, 2004; revised October 28, 2004.

The authors are with the Center for Self-Organizing and Intelligent Systems (CSOIS), Department of Electrical and Computer Engineering, Utah State University, Logan, UT 84322-4160 USA (e-mail: hyosung@cc.usu.edu; yqchen@ece.usu.edu; douhf@ece.usu.edu).

Digital Object Identifier 10.1109/TMAG.2004.840182

to guarantee the  $l_2$ -stability of the overall system; 2) from the second repetitive trajectory and onward, a trajectory-periodic adaptive compensator stabilizes the system; and 3) to make use of the stored past state-dependent cogging information, a search process is utilized for adapting the current cogging coefficient. The validity of our adaptive cogging and friction compensator is illustrated through numerical simulations based on an actual PMLM model.

The paper is organized as follows: In Section II, the system model and preliminary definitions are given and in Section III, a new adaptive state-dependent cogging and friction compensator is designed based on Lyapunov stability analysis. Simulation tests are performed in Section IV. Conclusions are given in Section V.

## II. SYSTEM MODEL AND STATE PERIODICITY

In this section, the dynamic equation of PMLM is presented and the state domain is defined, in which the PMLM has the trajectory periodicity. The cogging force of (2) can be written as  $-a(x)$ , where  $a(x)$  is the function of  $x$ . The Coulomb friction is simply modeled as

$$F_{\text{fric}} = -b\text{sgn}(v) \quad (3)$$

which is discontinuous at zero velocity. In this paper, the dynamics of a PMLM, which was introduced in [6], is slightly modified for ease of presentation of our main ideas without loss of generality. From [6, eqs. (1)–(3)], ignoring load and small disturbances such as  $F_{\text{load}}$  and  $F_n$ , and also ignoring the armature inductance  $L$  due to its small value compared to the resistance  $R$ , we derive a simple PMLM dynamic like

$$\ddot{x}(t) = -\frac{k_f k_e}{Rm} \dot{x} - \frac{1}{m} F_{\text{fric}} - \frac{1}{m} F_{\text{ripple}} + \frac{k_f}{Rm} u_v(t) \quad (4)$$

where  $u_v(t)$  and  $i(t)$  are time-varying motor terminal voltage and the armature current,  $x(t)$  is the motor position,  $R$  is the resistance,  $m$  is the moving mass,  $k_f$  is the force constant,  $k_e$  is the back electromotive force (EMF), and  $F_{\text{ripple}}$  is the position-dependent cogging force.

From now on, in this paper, let us use  $a(x)$  to denote the cogging force instead of using  $F_{\text{ripple}}$ , and it is supposed that coefficients  $k_f$ ,  $k_e$ ,  $m$ , and  $R$  are known from the motor technical specification sheet (these values can be found in [5, Table 1]). The following servo control problem is then considered:

$$\dot{x}(t) = v(t) \quad (5)$$

$$\dot{v}(t) = -\frac{p}{m}v - \frac{1}{m}a(x) - \frac{1}{m}b\text{sgn}(v) + u \quad (6)$$

where  $x$  is the position,  $a(x)$  is the unknown position-dependent cogging disturbance [i.e.,  $F_{\text{ripple}}$  in (4)],  $b$  is the unknown friction coefficient,  $v$  is the velocity,  $u$  is the control input ( $u := (k_f/Rm)u_v(t)$ ), and  $p := k_f k_e/R$ .

First, before proceeding to present our main results, the following definitions and assumptions are necessary.

*Definition 2.1:* The total passed trajectory is given as

$$s = \int_0^t \frac{|dx|}{d\tau} d\tau = \int_0^t |v(\tau)| d\tau$$

where  $x$  is the position, and  $v$  is the velocity. In [20], it was defined as the curvilinear abscissa associated with the trajectory of the relative motion. In our definition, since  $s$  is the summation of absolute position increase along the time axis,  $s$  is a monotonously growing signal. Physically it is the total passed trajectory; hence, it has the following property:

$$s(t_1) \geq s(t_2), \quad \text{iff } t_1 \geq t_2.$$

With notation  $s$ , the position corresponding to  $s(t)$  is denoted as  $x(s)$  and the cogging force corresponding to  $s(t)$  is denoted as  $a(s)$ .

*Definition 2.2:* Since the cogging force arises as a result of the mutual attraction between the magnets and cores of the translator, the cogging force is periodic with respect to position [5]. Based on Definition 2.1, the following relationship is derived:

$$a(s) = a(s - s_p), \quad \text{and } x(s) = x(s - s_p) \quad (7)$$

where  $s_p$  is periodicity of the trajectory.

*Definition 2.3:* In Definition 2.2,  $s_p$  was defined as periodic trajectory. So,  $s(t) - s_p$  is one trajectory past point from  $x(t)$  on the  $s$  axis. Let us denote the time corresponding to  $x(t) - s_p$  with  $T_t$ . Then,  $t - T_t$  is the time elapse to complete one periodic trajectory from the time  $T_t$  to time  $t$ . This time elapse is called a ‘‘cycle.’’ Particularly, it is called a ‘‘trajectory cycle’’ at time  $t$  and denoted as  $P_t$ . So,  $P_t = t - T_t$ . It is called ‘‘the search process’’ to find  $P_t$  at time instant  $t$  (note: the search process can be performed by interpolation).

*Assumption 2.1:* Throughout the paper, it is assumed that the current position and current time of the PMLM are measured and  $T_t$  is always calculated. Hence,  $P_t$  is calculated at current time instant  $t$ .

With the above definitions and assumption, the following property is observed.

*Property 2.1:*

$$x(t) = s(t) - m's_p \quad (8)$$

where  $m'$  is the integer part of  $s(t)/s_p$ .

*Remark 2.1:* As will be shown in Section III, for ease of implementation, the actual state-dependent cogging force  $a(s(t))$  is not estimated on the state axis although in theory we can do so. Instead,  $a(t)$  is estimated on the time axis. So, to find  $a(s(t) - s_p)$ , the following formula is used:

$$a(s(t) - s_p) = a(t - P_t). \quad (9)$$

Here,  $P_t$  is calculated in Assumption 2.1 (recall that  $P_t$  can be used to indicate exactly one-trajectory past position).

From (8) and (9), we also have the following property.

*Property 2.2:* The current cogging force is equal to one-trajectory past cogging force. From the relationship

$$\begin{aligned} a(s(t) - s_p) &= a(x(t) + m's_p - s_p) \\ &= a(x(t)) \\ &= a(t - P_t) \end{aligned} \quad (10)$$

the following equality is derived:  $a(x(t)) = a(t - P_t)$ .

Now, based on the above discussions, the following stability analysis is performed in this paper. Our compensation approach is summarized as follows.

- When  $s(t) < s_p$ , the system is controlled to be bounded input bounded output (in  $l_2$ -norm).
- When  $s(t) \geq s_p$ , the system is stabilized to follow the desired speed at the desired position. By a trajectory periodic adaptation, the unknown external disturbances (the summation of the cogging and friction forces) are estimated.

The following notations are used:

$$\begin{aligned} e_x(t) &= x(t) - x_d(t); & e_v &= v(t) - v_d(t); \\ e_a(s(t)) &= a(s(t)) - \hat{a}(s(t)); & e_b(t) &= b - \hat{b}(t) \end{aligned}$$

where  $x_d(t)$  is the desired position,  $v_d(t)$  is the desired velocity,  $\hat{a}(s(t))$  is the estimated cogging force,  $\hat{b}(t)$  is the estimated friction coefficient, and  $\hat{a}(s(t)) = \hat{a}(t)$ . Here, we can change  $e_a(s(t)) = a(s(t)) - \hat{a}(s(t))$  into time domain such as

$$\begin{aligned} e_a(s(t)) &= a(s(t)) - \hat{a}(s(t)) \\ &= a(t) - \hat{a}(t) \\ &= e_a(t). \end{aligned} \quad (11)$$

In the same way, the following relationships are true:

$$\begin{aligned} e_b(s(t)) &= e_b(t); & x(s(t)) &= x(t); & x_d(s(t)) &= x_d(t); \\ v_d(s(t)) &= v_d(t); & v(s(t)) &= v(t). \end{aligned}$$

The control objective is to track or servo the given desired position  $x_d(t)$  and the corresponding desired velocity  $v_d(t)$  with tracking errors as small as possible. In practice, it is reasonable to assume that  $x_d(t)$ ,  $v_d(t)$ , and  $\dot{v}_d(t)$  are all bounded. In the next section, based on relationship  $a(x(t)) = a(t - P_t) = a(t)$ ,  $a(x(t))$  is equivalent to  $a(t)$  as in (11). So,  $a(x)$  can be replaced by  $a(t)$ .

### III. STATE-DEPENDENT ADAPTIVE COGGING COMPENSATION

In this section, the state-periodic external disturbance is compensated based on Lyapunov stability analysis. The feedback controllers are designed as follows. When  $s \geq s_p$

$$u = \frac{\hat{a}(t) + \hat{b}\text{sgn}(v(t))}{m} + \frac{p}{m}v + \dot{v}_d(t) - \alpha S(t) - \lambda e_v(t) \quad (12)$$

and when  $s < s_p$

$$u = \frac{\hat{a}(t)}{m} + \frac{p}{m}v + \dot{v}_d(t) - \eta e_x(t) - \lambda e_v(t) \quad (13)$$

with

$$S(t) := e_v(t) + \lambda e_x(t) \quad (14)$$

where  $\alpha$  and  $\lambda$  are positive gains,  $\hat{a}(t)$  is an estimated cogging force from an adaptation mechanism to be specified later,  $\hat{b}$  is the

estimated friction coefficient,  $\dot{v}_d(t)$  is the desired acceleration, and  $e_x(t) = x(t) - x_d(t)$  is the position tracking error. Also remember that  $e_x(s(t)) = e_x(t)$  and  $S(s(t)) = S(t)$ .

Our adaptation law is designed as follows:

$$\hat{a}(t) = \begin{cases} \hat{a}(t - P_t) - \frac{K}{m}S(t), & \text{if } s \geq s_p \\ z - g(v), & \text{if } s < s_p \end{cases} \quad (15)$$

$$\dot{\hat{b}}(t) = \begin{cases} -\frac{S(t)}{m}\text{sgn}(v), & \text{if } s \geq s_p \\ 0, & \text{if } s < s_p \end{cases} \quad (16)$$

where  $\hat{a}(t - P_t) = \hat{a}(s - s_p)$  (note:  $P_t$  is the trajectory cycle defined in Definition 2.3),  $P_1$  is the first trajectory cycle specified in Definition 3.1,  $K$  is a positive design parameter (it is called the periodic adaptation gain),  $z$  will be defined in the following paragraph, and  $g(v)$  is a tuning function to be selected later based on certain guidelines.

*Definition 3.1:* The first trajectory cycle  $P_1$  is the elapsed time to complete the first repetitive trajectory cycle from the initial starting time  $t_0$ . In other words,  $P_1$  is the time corresponding to the total passed trajectory when  $s(t) = s_p$ .

In our analysis part, the following tuning function property is required for  $g(v)$ :

$$0 < g'(v) < \infty \quad (17)$$

where  $g'(\cdot) = \partial g(\cdot)/\partial \cdot$ ; and the following tuning mechanism is required for  $z$ :

$$\dot{z} = g'(v)[\dot{v}_d - \eta e_x - \lambda e_v] - \frac{e_v}{m}. \quad (18)$$

The above tuning function design will be given later.

Consider two cases: 1) when  $0 \leq t < P_1$  ( $0 \leq s \leq s_p$ ) and 2) when  $t \geq P_1$  ( $s \geq s_p$ ). The key idea is that, for case 1), it is required to show the finite time boundedness of equilibrium points. For case 2), it is necessary to show the stability or asymptotic stability of equilibrium points in the sense of Lyapunov. Let us investigate case 2) first. Our major results are summarized in the following theorems with Remark 3.1.

*Remark 3.1:* From the relationship (11), it can be said that if  $e_a(t) \rightarrow 0$  as  $t \rightarrow \infty$ , then  $e_a(s) \rightarrow 0$  as  $s \rightarrow \infty$ . Thus, in what follows, the stability analysis of  $a(x)$  is performed on the time axis.

*Theorem 3.1:* When  $t \geq P_1$  ( $s \geq s_p$ ), the control law (12) and the periodic adaptation laws (15) and (16) guarantee the stability of the equilibrium points  $e_x(t)$ ,  $e_v(t)$ ,  $e_a(t)$ , and  $e_b(t)$  as  $t \rightarrow \infty$  ( $s \rightarrow \infty$ ).

*Proof:* See the Appendix for the proof. ■

The above theorem only guarantees the stability property in the sense of Lyapunov. To explore the asymptotical stability, the following notation and lemma are provided. The total external disturbances including cogging force and friction force are denoted as

$$c(t) = \frac{a(t) + b\text{sgn}(v)}{m}$$

and the corresponding error is denoted as

$$\begin{aligned} e_c(t) &= \frac{1}{m} [a(t) + b\text{sgn}(v) - \hat{a}(t) - \hat{b}\text{sgn}(v)] \\ &= \frac{e_a(t) + e_b\text{sgn}(v)}{m}. \end{aligned} \quad (19)$$

*Lemma 3.1:* In the following equation with initial state  $x(0) = x_0 = 0$

$$y = \dot{x} + \tau x, \quad \tau > 0$$

$y \rightarrow 0$  as  $t \rightarrow \infty$  if and only if  $x \rightarrow 0$  as  $t \rightarrow \infty$ .

*Proof:* The sufficient condition is immediate because  $x = 0$  makes  $y = 0$ . The necessary condition is proved easily by calculating the solution. When  $y = 0$ ,  $x(t)$  is calculated as

$$x(t) = x_0 + e^{-\tau t}.$$

So, if  $x_0 = 0$ , as  $t \rightarrow \infty$ ,  $x(t) \rightarrow 0$ . ■

Now, let us consider the asymptotically stability condition of the equilibrium points  $e_x$ ,  $e_v$ , and  $e_c$  in the following theorem.

*Theorem 3.2:* If the initial position ( $x_0$ ) is at the desired initial position ( $x_d(0)$ ), i.e.,  $e_x(0) = 0$ , the control law (13) and the periodic adaptation law (15) guarantee the asymptotically stability of the equilibrium points:  $e_x$ ,  $e_v$ , and  $e_c$  as  $t \rightarrow \infty$  ( $t \geq P_1$ , or  $s \geq s_p$ ).

*Proof:* See the Appendix for the proof. ■

*Remark 3.2:* The asymptotical stability of  $e_c$  does not guarantee the asymptotical stability of  $e_a$  and  $e_b$ . In other words, even if the suggested theorem guarantees the asymptotical stability of  $e_x$  and  $e_v$ , it does not provide the asymptotical stability of  $e_a$  and  $e_b$ . However, the cogging disturbance and friction disturbance will still be compensated altogether successfully by Theorem 3.2.

Now, let us consider the case 1) when  $t < P_1$  ( $s \leq s_p$ ) and the overall stability when  $t \geq 0$  ( $s \geq 0$ ).

*Theorem 3.3:* If  $\dot{a}$  and  $b$  are bounded, the equilibrium points of  $e_x$ ,  $e_v$ ,  $e_a$ , and  $e_b$  are stable (or  $e_c$  is asymptotically stable) as  $t \rightarrow \infty$  ( $s \rightarrow \infty$ ).

*Proof:* See the Appendix for the proof. ■

In this section, the state-periodic adaptive controller was designed to compensate the state-periodic cogging and friction forces. In next section, simulation tests are performed based on the suggested theorems of this section.

#### IV. SIMULATION ILLUSTRATIONS

To verify the suggested method, two different simulation tests are performed. The first test is to compensate the high-order Fourier expansion of the cogging force and the second test is to check the robustness of the suggested method against the model uncertainty.

##### A. Compensation of the High-Order Cogging Force

For this simulation test, let us use the following reference position and velocity signals, which have the same period and amplitude as in [5, Fig. 2]:

$$\begin{aligned} x_d(t) &= 0.25 \sin\left(2\pi \frac{t}{T_d} - \frac{\pi}{2}\right) + 0.25 \\ v_d(t) &= 0.5\pi \frac{1}{T_d} \cos\left(2\pi \frac{t}{T_d} - \frac{\pi}{2}\right) \\ \dot{v}_d(t) &= -0.25 \left(2\pi \frac{1}{T_d}\right)^2 \sin\left(2\pi \frac{t}{T_d} - \frac{\pi}{2}\right) \end{aligned} \quad (20)$$

where  $T_d = 4$  s. To check our method, the actual PMLM model is used in the simulation. We use actual parameter values of

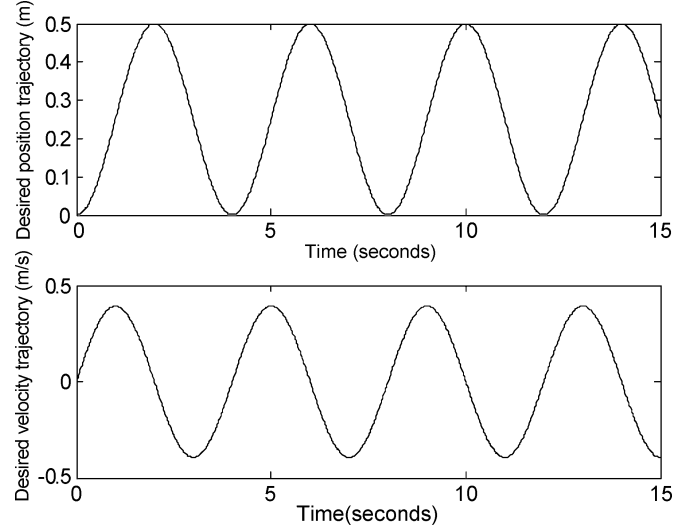


Fig. 1. Top: desired position trajectory. Bottom: desired velocity trajectory.

LD-3810 PMLM motor, which are given in [5, Table 1]. Furthermore, to represent the realistic friction model, the following friction force is used in simulation:

$$F_{\text{fric}} = \left[ f_c + (f_s - f_c) e^{\left(\frac{v}{v_s}\right)^2} + f_v v \right] \text{sgn}(v) \quad (21)$$

where  $f_c$  is Coulomb friction coefficient ( $b$  in analysis),  $f_s$  is static friction coefficient,  $f_v$  is the viscous friction coefficient, and  $v_s$  is the lubricant parameter. In (4), parameter values are given as  $m = 5.4$  kg;  $R = 16.8$  ohms;  $k_f = 130$  N/A; and  $k_e = 123$  V/m/s. (same values as used in [5]). As for friction force, the simulated parameter values are  $f_c = 10$ ,  $f_s = 20$ ,  $v_s = 0.1$ , and  $f_v = 10$  (same values as used in [5]). The control gains in (12) and (13) were selected as  $\alpha = 50$ ,  $\lambda = 20$ , and  $\eta = 20$ ; and  $g(v)$  was designed as  $40v$  to satisfy (17). In (15), the periodic adaptation gain  $K$  was selected as 1000. To represent the high-order Fourier expansion, the following cogging force was modeled:

$$F_{\text{cogging}} = A_1 \sin(\omega x) + A_2 \sin(3\omega x) + A_3 \sin(5\omega x) \quad (22)$$

where  $A_1 = 8.5$ ,  $\omega = 314$  rad/m (same values as used in [5]),  $A_2 = 4.25$ , and  $A_3 = 2.0$ . Recall that [5] only used first-order Fourier expansion in simulation, but our cogging force model includes higher order Fourier expansions.

At the top of Fig. 1 is the desired position on the time axis, and at the bottom is the desired velocity. Note that we used the same desired trajectory as used in [5]. Fig. 2 shows the position tracking error where the  $Y$  axis of the top subfigure ranges from 0.02 to  $-0.02$  m while the  $Y$  axis of the bottom subfigure ranges from 0.002 to  $-0.002$  m. As shown in the top subfigure of Fig. 2, after the first repetitive trajectory, the tracking error was significantly reduced. When the bottom subfigure of Fig. 2 is compared with [5, Fig. 3], it is observed that our result is slightly better than the result of [5] (i.e., in [5], the position error is about 0.002 m, while Fig. 2 shows less than 0.001 m error after 5 s). Furthermore, from the fact that we have included high-order Fourier terms of the cogging force, our method is superior to the existing method for compensating the actual state-dependent cogging force. Fig. 3 shows our adaptive control input signal. Comparing Fig. 3 with [5, Fig. 3], we found that the required

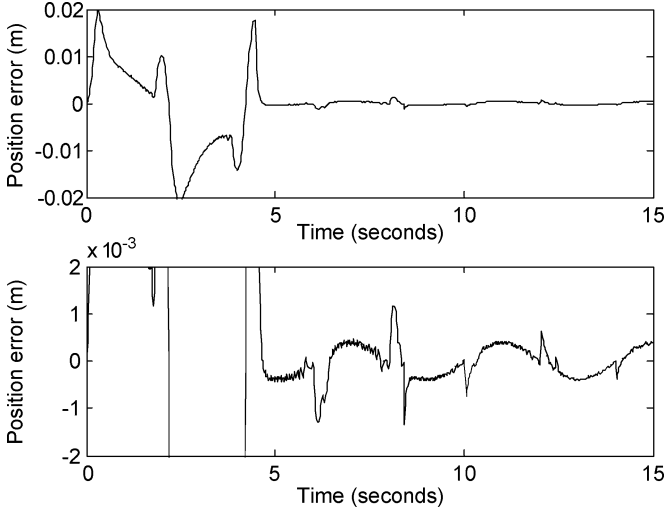


Fig. 2. Top: position tracking error. Bottom: position tracking error zoomed.

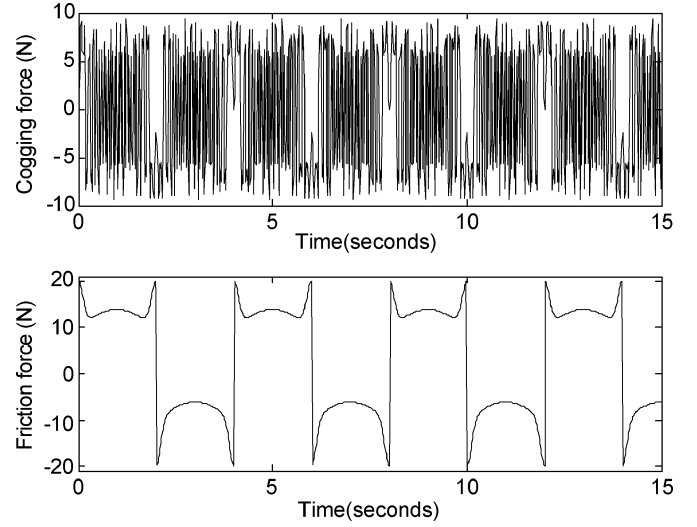


Fig. 4. Top: true cogging force from the model (22). Bottom: true friction force from the model (21).

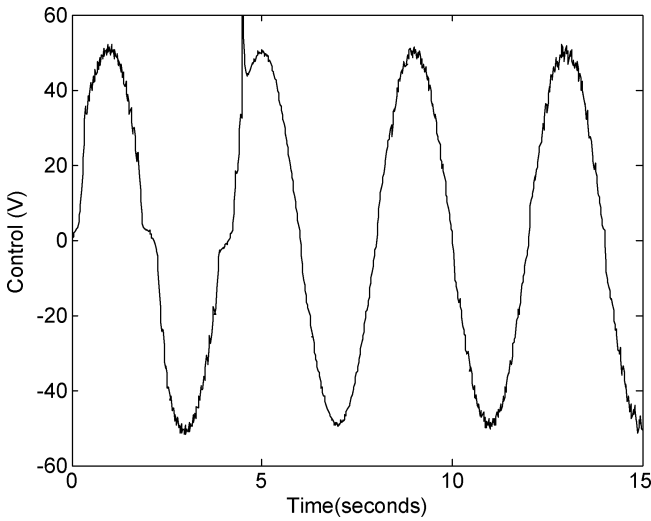


Fig. 3. Adaptive control input signal.

control input of our system is slightly less than the required control input of [5] (i.e., in [5], the control force is about 75 V, while Fig. 3 shows that about 50 V are required in our case). The top subfigure of Fig. 4 is the cogging force from the simulation model (22) with respect to the  $x_d$ . The bottom subfigure of Fig. 4 is the friction force signal using the model (21). These signals are the “true” actual forces experienced by the PMLM. For a comparison, with our adaptive control method, the estimated cogging force and friction force time histories are shown in the top and bottom subfigure of Fig. 5, respectively. From Figs. 4 and 5, we can observe a good agreement except in the initial transient phase.

We should note that the reason that the tracking errors are not perfectly zero is mainly due to the mismatched frictional model used in the simulation (21) compared to the simple model (3). Of course, given the more complicated frictional model (21), we can design adaptive compensation scheme accordingly, but this is beyond the scope of this paper.

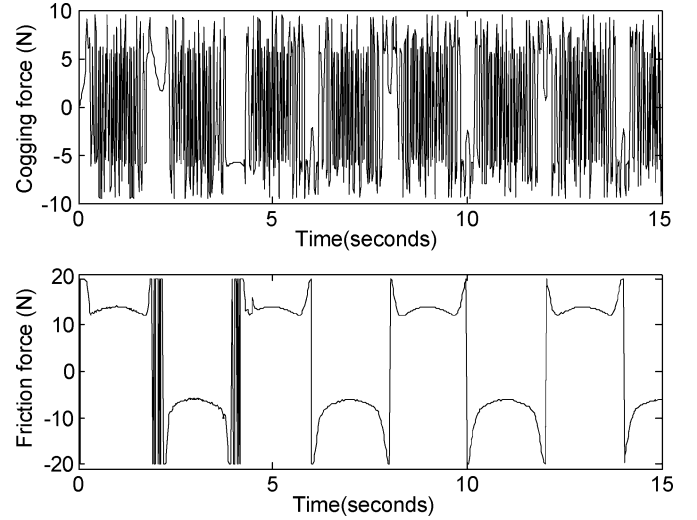


Fig. 5. Top: estimated cogging force. Bottom: estimated friction force.

### B. Robustness Test of the Suggested Method

For the robustness test of the suggested method, in the PMLM model of (4), 10% model uncertainties are assumed as

$$\begin{aligned} R' &= R + 0.1wR; & m' &= m + 0.1wm; \\ k'_f &= k_f + 0.1wk_f; & k'_e &= k_e + 0.1wk_e \end{aligned}$$

where  $R$ ,  $m$ ,  $k_f$ , and  $k_e$  are nominal resistance, mass, force constant, and back EMF, respectively;  $R'$ ,  $m'$ ,  $k'_f$ , and  $k'_e$  are perturbed values; and  $w$  is the random number in the range of  $-1 \leq w \leq 1$ . For the reliable test, 20 different Monte Carlo type random tests are performed just for qualitative justification. Fig. 6 shows the test results. As shown in the figure, we observe that the suggested method is robust against the model uncertainties and the tracking performance is still acceptable. Therefore, we conclude that the closed-loop system designed by the suggested method provides the reliable robustness against the model uncertainties or parameter perturbations.

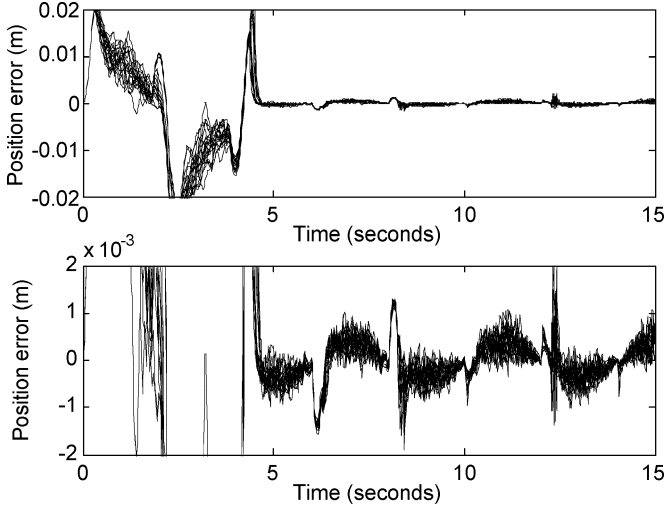


Fig. 6. With 10% model uncertainties. Top: position tracking error. Bottom: position tracking error zoomed.

## V. CONCLUSION

In this paper, a new cogging and friction force compensation method for the PMLM has been proposed when the PMLM is commanded to execute a given task repeatedly. The key idea of our method is to use the periodicity of the cogging disturbance, which is dependent on the position. From the one past trajectory information, the current adaptation law was updated. Even though the stability analysis was performed on the time axis, the position-dependent cogging disturbance can be successfully compensated on the state-axis. It is believed that the suggested method can be effectively used in many real applications such as satellite, trail system, and factory process control. Note that although the state-periodic adaptive control method was developed for compensating cogging disturbance, the key ideas of our method can be modified to compensate other state-dependent nonlinear disturbances of a general shape. From the simulation results, we can conclude that our proposed control method works effectively when the cogging force is represented in the form of high-order Fourier expansion. Furthermore, compared to the reported results, we observe that, even with extra order Fourier expansion terms in the cogging force, our method requires less control effort and achieves smaller position tracking error. In summary, the position-dependent external disturbance such as cogging force can be successfully compensated by using the trajectory periodicity of the state-dependent disturbance.

## APPENDIX I PROOFS OF THEOREMS

*Proof:* (Theorem 3.1) Consider the following Lyapunov-like function at  $s(t)$ , whose corresponding time is  $t$ :

$$V(t) = \frac{1}{2} (e_b(t))^2 + \frac{1}{2} S^2(t) + \frac{1}{2K} \int_{t-P_t}^t e_a^2(\tau) d\tau \quad (23)$$

where  $P_t$  is calculated by the search process as commented in Definition 2.3. Then, from (23), the difference of the positive

Lyapunov-like functions at two discrete time points (note: time difference is  $P_t$ ) can be calculated as

$$\begin{aligned} \Delta V(t) &= V(t) - V(t - P_t) \\ &= \frac{1}{2} (e_b(t))^2 - \frac{1}{2} (e_b(t - P_t))^2 \\ &\quad + \frac{1}{2} S^2(t) - \frac{1}{2} S^2(t - P_t) \\ &\quad + \frac{1}{2K} \int_{t-P_t}^t [e_a^2(\tau) - e_a^2(\tau - P_\tau)] d\tau \\ &= \int_{t-P_t}^t [e_b(\tau) \dot{e}_b(\tau) + S(\tau) \dot{S}(\tau)] d\tau \\ &\quad + \frac{1}{2K} \int_{t-P_t}^t [e_a^2(\tau) - e_a^2(\tau - P_\tau)] d\tau \\ &= \int_{t-P_t}^t [e_b(\tau) \dot{e}_b(\tau) + S(\tau) \dot{S}(\tau)] d\tau \\ &\quad + \frac{1}{2K} \int_{t-P_t}^t [e_a^2(\tau) - e_a^2(\tau - P_\tau)] d\tau. \quad (24) \end{aligned}$$

To simplify our presentation, let the first integral term on the right-hand side be denoted by  $A$  and the second integral term by  $B$ . That is

$$\begin{aligned} A &:= \int_{t-P_t}^t [e_b(\tau) \dot{e}_b(\tau) + S(\tau) \dot{S}(\tau)] d\tau; \\ B &:= \frac{1}{2K} \int_{t-P_t}^t [e_a^2(\tau) - e_a^2(\tau - P_\tau)] d\tau. \end{aligned}$$

Here, from  $a(s - s_p) = a(t - P_t)$  in Remark 2.1, the following equalities are satisfied:

$$a(s - s_p) = a(t - P_t) = a(t) = a(s).$$

Then, by several algebraic calculations and using  $a(t - P_t) = a(t)$ ,  $B$  can be changed to

$$\begin{aligned} B &= \frac{1}{2K} \int_{t-P_t}^t [a(\tau) - \hat{a}(\tau)]^2 \\ &\quad - [a(\tau - P_\tau) - \hat{a}(\tau - P_\tau)]^2 d\tau \\ &= \frac{1}{2K} \int_{t-P_t}^t \{ \hat{a}(\tau - P_\tau) - \hat{a}(\tau) \} \\ &\quad \times \{ 2[a(\tau) - \hat{a}(\tau)] + [\hat{a}(\tau) - \hat{a}(\tau - P_\tau)] \} d\tau \\ &= \frac{1}{2K} \int_{t-P_t}^t \beta(\tau) \{ 2[a(\tau) - \hat{a}(\tau)] - \beta(\tau) \} d\tau \quad (25) \end{aligned}$$

where

$$\beta(\tau) := \hat{a}(\tau - P_\tau) - \hat{a}(\tau).$$

By applying (15), we have  $\beta(t) = (K/m)S(t)$ . Furthermore, using (6), (12), and

$$\begin{aligned} \dot{e}_x &= \dot{x} - \dot{x}_d = e_v, \\ \dot{e}_v &= \dot{v} - \dot{v}_d \\ &= -\frac{p}{m}v - \frac{1}{m}a(t) - \frac{1}{m}b\text{sgn}(v) + u - \dot{v}_d \\ &= \frac{1}{m} \left( -a(t) - b\text{sgn}(v) + \hat{a}(t) + \hat{b}\text{sgn}(v) \right) \\ &\quad - \alpha S(t) - \lambda e_v(t) \\ &= \frac{-e_a(t) - e_b\text{sgn}(v)}{m} - \alpha S(t) - \lambda e_v(t) \end{aligned} \quad (26)$$

from (14)

$$\begin{aligned} \dot{S} &= \dot{e}_v + \lambda \dot{e}_x(t) \\ &= \frac{-e_a(t) - e_b\text{sgn}(v)}{m} - \alpha S(t) - \lambda e_v(t) + \lambda e_v(t) \\ &= \frac{-e_a - e_b\text{sgn}(v)}{m} - \alpha S(t). \end{aligned} \quad (27)$$

Then, using

$$\dot{e}_b = \dot{b} - \dot{\hat{b}} = -\dot{\hat{b}} \quad (28)$$

$A$  can be expressed as

$$A = \int_{t-P_t}^t -e_b(\tau)\dot{\hat{b}} + S(\tau) \left[ \frac{-e_a(\tau) - e_b(\tau)\text{sgn}(v)}{m} - \alpha S(\tau) \right] d\tau. \quad (29)$$

Thus,  $\Delta V$  becomes

$$\begin{aligned} \Delta V &= A + B \\ &= \int_{t-P_t}^t -e_b(\tau)\dot{\hat{b}} \\ &\quad + S(\tau) \left[ \frac{-e_a(\tau) - e_b(\tau)\text{sgn}(v)}{m} - \alpha S(\tau) \right] d\tau \\ &\quad + \frac{1}{2K} \int_{t-P_t}^t \beta \{2[a(\tau) - \hat{a}(\tau)] - \beta(\tau)\} d\tau. \end{aligned} \quad (30)$$

Also, using  $e_a(t) = a(t) - \hat{a}(t)$ ,  $A + B$  is changed to

$$\begin{aligned} A+B &= \int_{t-P_t}^t -e_b(\tau)\dot{\hat{b}} - \frac{S(\tau)e_b(\tau)\text{sgn}(v)}{m} \left[ -\alpha S^2 - \frac{1}{2K}\beta^2 \right] d\tau \\ &\quad + \int_{t-P_t}^t \left[ -\frac{e_a(\tau)}{m}S(\tau) + \frac{\beta}{K}e_a(\tau) \right] d\tau. \end{aligned} \quad (31)$$

Furthermore, from (15), using  $S(\tau) = (m/K)\beta(\tau)$ , since the second term of the right-hand side of the preceding equation is deleted, we have

$$A+B = \int_{t-P_t}^t \left[ -e_b(\tau)\dot{\hat{b}} - \frac{S(\tau)e_b(\tau)\text{sgn}(v)}{m} - \alpha S^2 - \frac{1}{2K}\beta^2 \right] d\tau. \quad (32)$$

Then, using  $\dot{\hat{b}} = -S(t)\text{sgn}(v)/m$  from (16)

$$\begin{aligned} A+B &= \int_{t-P_t}^t \left( -\alpha S^2 - \frac{1}{2K}\beta^2 \right) d\tau \\ &= \int_{t-P_t}^t \left( -\alpha S^2 - \frac{K}{2m}S^2 \right) d\tau. \end{aligned} \quad (33)$$

Therefore, since  $\Delta V(t) \leq 0$ , the proof is completed.  $\blacksquare$

*Proof:* (Theorem 3.2) Here, LaSalle's invariant set theorem is used to prove the asymptotical stability. From (33), only  $S = 0$  makes  $\Delta V = 0$ . Using the definition  $S = e_v + \lambda e_x$  and relationship  $e_v = \dot{e}_x$ , we have

$$S = e_v + \lambda e_x = \dot{e}_x + \lambda e_x. \quad (34)$$

So, from Lemma 3.1, if  $e_x(0) = 0$ , only  $e_x = 0$  makes  $S = 0$ . Also, since  $e_x = 0$ , we have  $e_v = 0$  from  $e_v + \lambda e_x = 0$ . Therefore,  $e_x$  and  $e_v$  are asymptotically stable at equilibrium points. Now, let us consider  $e_c$  in what follows. From (27),  $\dot{S} = ((-e_a - e_b\text{sgn}(v))/m) - \alpha S = -e_c - \alpha S$ ,  $\dot{S} = -e_c$  because  $S = 0$ . Then, by showing that  $\dot{S} \rightarrow 0$  as  $S \rightarrow 0$ ,  $e_c = 0$  can be an asymptotical stable point. Our approaches are as follows. From the following definition:

$$\dot{S} = \lim_{\Delta t \rightarrow 0} \frac{S(t + \Delta t) - S(t)}{\Delta t} \quad (35)$$

we know that as  $t \rightarrow \infty$ ,  $S(t + \Delta t) \rightarrow 0$ , and  $S(t) \rightarrow 0$ . However, from our original assumption of the periodicity such as  $\Delta t = P_t$ , if  $P_t$  is not zero, then  $\Delta t \neq 0$ , while  $S(t + \Delta t) - S(t) \rightarrow 0$  as  $t \rightarrow \infty$ . Thus, in (35),  $\dot{S} \rightarrow 0$  as  $t \rightarrow \infty$ , hence  $-e_c \rightarrow 0$  as  $t \rightarrow \infty$ . However, if  $-e_c \neq 0$ ,  $\dot{S} \neq 0$ . Then  $S(t + \Delta t) - S(t) \neq 0$ , which is a contradiction to  $S(t + \Delta t) - S(t) = 0$ . Therefore, it can be concluded that only  $-e_c = 0$  makes  $\dot{S} = 0$  and in the sequel, no trajectory can stay except  $e_c = 0$  when  $S = 0$ . Since only  $e_x = 0$ ,  $e_v = 0$ , and  $e_c = 0$  make  $S = 0$ , from the invariant set theorem, the equilibrium points  $e_x$ ,  $e_v$ , and  $e_c$  are asymptotically stable. This completes the proof of this theorem.  $\blacksquare$

*Proof:* (Theorem 3.3) In this case, let us use the following Lyapunov function:

$$V(t) = \frac{\eta}{2}e_x^2(t) + \frac{1}{2}e_v^2(t) + \frac{1}{2}e_a^2(t) + \frac{1}{2}e_b^2. \quad (36)$$

Then, the derivative of  $V$  is expressed by using (6) as

$$\begin{aligned} \dot{V}(t) &= \eta e_x \dot{e}_v + e_v \left( -\frac{p}{m}v - \frac{1}{m}a(t) - \frac{1}{m}b\text{sgn}(v) + u - \dot{v}_d \right) \\ &\quad + e_a \dot{e}_a + e_b \dot{e}_b. \end{aligned} \quad (37)$$

From (13), (15), (16), and (18), using

$$\begin{aligned}\dot{e}_b &= \dot{b} - \dot{b} = 0 \\ u &= \frac{1}{m}\hat{a}(t) + \frac{p}{m}v + \dot{v}_d(t) - \eta e_x(t) - \lambda e_v(t) \\ \dot{e}_a &= \dot{a} - \dot{\hat{a}} = \dot{a} - \dot{z} + g'(v)\dot{v}\end{aligned}$$

we have

$$\begin{aligned}\dot{V}(t) &= \eta e_x e_v + e_v \left[ \frac{-a(t) - b \operatorname{sgn}(v) + \hat{a}(t)}{m} \right] \\ &\quad + e_v [\dot{v}_d(t) - \eta e_x(t) - \lambda e_v(t) - \dot{v}_d] \\ &\quad + e_a [\dot{a} - \dot{z} + g'(v)\dot{v}].\end{aligned}\quad (38)$$

Now, rewriting  $\dot{v}$  of (6) such as

$$\begin{aligned}\dot{v} &= \frac{-a(x) - b \operatorname{sgn}(v)}{m} - \frac{p}{m}v + u \\ &= \frac{-a(x) - b \operatorname{sgn}(v) + \hat{a}(t)}{m} + \dot{v}_d(t) - \eta e_x(t) - \lambda e_v(t) \\ &= \frac{-e_a - b \operatorname{sgn}(v)}{m} + \dot{v}_d(t) - \eta e_x(t) - \lambda e_v(t)\end{aligned}\quad (39)$$

and using (18), and inserting (39) into (38), (38) is changed to

$$\begin{aligned}\dot{V}(t) &= -\lambda e_v^2 - \frac{b \operatorname{sgn}(v)}{m} e_v - \frac{1}{m} e_a e_v \\ &\quad + e_a \left[ \dot{a} + \frac{1}{m} e_v + g'(v) \left( \frac{-e_a - b \operatorname{sgn}(v)}{m} \right) \right] \\ &= -\lambda e_v^2 - \frac{1}{m} b \operatorname{sgn}(v) e_v - \frac{1}{m} e_a^2 g'(v) \\ &\quad - \frac{1}{m} e_a b g'(v) \operatorname{sgn}(v) + e_a \dot{a}.\end{aligned}\quad (40)$$

Let us investigate  $-\lambda e_v^2 - (1/m)b \operatorname{sgn}(v)e_v$  and  $-(1/m)e_a^2 g'(v) - (1/m)e_a b g'(v) \operatorname{sgn}(v) + e_a \dot{a}$  of (40) separately. The following relationship is derived:

$$\begin{aligned}-\lambda e_v^2 - \frac{1}{m} b \operatorname{sgn}(v) e_v &= -\lambda \left( e_v^2 + \frac{b \operatorname{sgn}(v)}{\lambda m} e_v \right) \\ &= -\lambda \left( e_v + \frac{b \operatorname{sgn}(v)}{2\lambda m} \right)^2 + \frac{b^2}{4\lambda m^2}\end{aligned}\quad (41)$$

and  $-(1/m)e_a^2 g'(v) + (\dot{a} - (1/m)b g'(v) \operatorname{sgn}(v))e_a$  is changed to

$$\begin{aligned}-\frac{g'(v)}{m} \left( e_a - \frac{m}{2g'(v)} \left( \dot{a} - \frac{b}{m} g'(v) \operatorname{sgn}(v) \right) \right)^2 \\ + \frac{m}{4g'(v)} \left( \dot{a} - \frac{b}{m} g'(v) \operatorname{sgn}(v) \right)^2.\end{aligned}\quad (42)$$

Hence, since

$$-\lambda e_v^2 - \frac{1}{m} b \operatorname{sgn}(v) e_v \leq \frac{b^2}{4\lambda m^2}$$

and

$$\begin{aligned}-\frac{1}{m} e_a^2 g'(v) + \left( \dot{a} - \frac{1}{m} b g'(v) \operatorname{sgn}(v) \right) e_a \\ \leq \frac{m}{4g'(v)} \left( \dot{a} - \frac{b}{m} g'(v) \operatorname{sgn}(v) \right)^2\end{aligned}$$

the derivative of Lyapunov function is upper bounded such as

$$\dot{V}(t) \leq \frac{b^2}{4\lambda m^2} + \frac{m}{4g'(v)} \left( \dot{a} - \frac{b}{m} g'(v) \operatorname{sgn}(v) \right)^2.$$

Thus, it concludes that  $\dot{V}$  is bounded when  $t < P_1(s < s_p)$  if  $\dot{a}$  and  $b$  are bounded. Consequently,  $V$  is bounded since  $\dot{V}$  is bounded. Therefore,  $e_x$ ,  $e_v$ ,  $e_a$ , and  $e_b$  are also bounded in  $l_2$  vector norm topology at  $t < P_1(s < s_p)$ . Furthermore, when  $t \geq P_1(s \geq s_p)$ , the equilibrium points of  $e_x$ ,  $e_v$ ,  $e_a$ , and  $e_b$  are all ( $e_c$  is asymptotically stable with  $e_x(0) = 0$ ) stable from (33); so the system (5), (6) can be (asymptotically with  $e_x(0) = 0$ ) stabilized by the control law (12), (13) and the adaptation law (15), (16) as  $t \rightarrow \infty$ . This completes the proof.  $\blacksquare$

#### ACKNOWLEDGMENT

The authors would like to thank the anonymous reviewers for their constructive comments which improved the presentation of this paper.

#### REFERENCES

- [1] C. S. Koh and J.-S. Seol, "New cogging torque reduction method for brushless permanent-magnet motors," *IEEE Trans. Magn.*, vol. 39, no. 6, pp. 3503–3506, Nov. 2003.
- [2] P. J. Hor, Z. Q. Zhu, D. Howe, and J. Rees-Jones, "Minimization of cogging force in a linear permanent-magnet motor," *IEEE Trans. Magn.*, vol. 34, no. 5, pp. 3544–3547, Sep. 1998.
- [3] R. J. Cruise and C. F. Landy, "Reduction of cogging forces in linear synchronous motors," in *Proc. IEEE AFRICON*, Cape Town, South Africa, Sep. 28–Oct. 1 1999, pp. 623–626.
- [4] P. Krishnamurthy and F. Khorrami, "Adaptive control of stepper motors without current measurements," in *Proc. Amer. Control Conf.*, Arlington, VA, Jun. 25–27, 2001, pp. 1563–1568.
- [5] K. K. Tan, S. N. Huang, and T. H. Lee, "Robust adaptive numerical compensation for friction and force ripple in permanent-magnet linear motors," *IEEE Trans. Magn.*, vol. 38, no. 1, pp. 221–228, Jan. 2002.
- [6] K. K. Tan, T. H. Lee, H. Dou, and S. Zhao, "Force ripple suppression in iron-core permanent-magnet linear motors using an adaptive dither," *J. Franklin Inst.*, vol. 341, pp. 375–390, 2004.
- [7] A. van Zyl and C. F. Landy, "Reduction of cogging forces in a tubular linear synchronous motor by optimizing the secondary design," in *Proc. IEEE AFRICON*, Oct. 2002, pp. 689–692.
- [8] S.-M. Yang, F.-C. Lin, and M.-T. Chen, "Micro-stepping control of a two-phase linear stepping motor with three-phase VSI inverter for high-speed applications," in *Proc. 38th IAS Annu. Meeting*, Oct. 2003, pp. 473–479.
- [9] B. Friedland and Y.-J. Park, "On adaptive friction compensation," in *Proc. 30th IEEE Conf. Decision and Control*, Brighton, U.K., Dec. 1991, pp. 2899–2902.
- [10] B. Friedland and S. Mentzelopoulou, "On adaptive friction compensation without velocity measurement," in *Proc. 1st IEEE Int. Conf. Control Applications*, Dayton, OH, Sep. 1992, pp. 1076–1081.
- [11] T. Kubo, G. Anwar, and M. Tomizuka, "Application of nonlinear friction compensation to robot arm control," in *Proc. IEEE Int. Conf. Robotics and Automation*, Apr. 1986, pp. 722–727.
- [12] C. C. de Wit, P. Noel, A. Aubin, B. Brogliato, and P. Drevet, "Adaptive friction compensation in robot manipulators: low-velocities," in *Proc. IEEE Conf. Robotics and Automation*, Scottsdale, AZ, May 14–19, 1989, pp. 1352–1357.
- [13] D. A. Haessig, Jr and B. Friedland, "On the modeling and simulation of friction," in *Proc. Amer. Control Conf.*, San Diego, CA, May 23–25, 1990, pp. 1256–1261.
- [14] C. C. de Wit and V. Seront, "Robust adaptive friction compensation," in *Proc. IEEE Conf. Robotics and Automation*, Cincinnati, OH, May 13–18, 1990, pp. 1383–1388.

- [15] D. W. Vos, L. Valavani, and A. H. Flotow, "Intelligent model reference nonlinear friction compensation using neural networks and Lyapunov based adaptive control," in *Proc. IEEE Int. Symp. Intelligent Control*, Arlington, VA, Aug. 13–15, 1991, pp. 417–422.
- [16] A. Yazdizadeh and K. Khorasani, "Adaptive friction compensation based on the Lyapunov scheme," in *Proc. IEEE Int. Conf. Control Applications*, Dearborn, MI, Sep. 1996, pp. 1060–1065.
- [17] T.-L. Liao and T.-I. Chien, "An exponentially stable adaptive friction compensator," *IEEE Trans. Automat. Contr.*, vol. 45, no. 5, pp. 977–980, May 2000.
- [18] T. Zhang and M. Guay, "Comments on an exponentially stable friction compensator," *IEEE Trans. Automat. Contr.*, vol. 46, no. 11, pp. 1844–1845, Nov. 2001.
- [19] H.-S. Ahn and Y. Chen, "Time periodical adaptive friction compensation," in *Proc. IEEE Int. Conf. Robotics and Biomimetics (RoBio04)*, Shenyang, China, Aug. 22–26, 2004.
- [20] C. C. de Wit and L. Praly, "Adaptive eccentricity compensation," in *Proc. 37th IEEE Conf. Decision and Control*, Tampa, FL, Dec. 1998, pp. 2271–2276.

**Hyo-Sung Ahn** (S'04) received the B.S. and M.S. degrees in astronomy and space science from Yonsei University, Seoul, Korea, in 1998 and 2000, respectively, and the M.S. degree in electrical engineering from the University of North Dakota, Grand Forks, in 2003. Currently, he is pursuing the Ph.D. degree in electrical and computer engineering from Utah State University, Logan. His Ph.D. research topics are robust iterative learning control, periodic adaptive learning control, and parameter distributed system using iterative learning control.

In 2000, he joined ETRI, Korea, as an Assistant Researcher. From 2000 to 2001, he was with Attitude Control and Orbit Subsystem Group of KOMPSAT-2 in Korea Aerospace Industries, LTD as a research engineer, and from 2002 to 2003, he developed sensor fusion subsystem of the airborne imaging system using DGPS and IMU at the Upper Midwest Aerospace Consortium, North Dakota.

**YangQuan Chen** (S'95–SM'98) received the B.S. degree in industrial automation from the University of Science and Technology of Beijing (USTB), Beijing, China, in 1985, the M.S. degree in automatic control from Beijing Institute of Technology (BIT) in 1989, and the Ph.D. degree in control and instrumentation from Nanyang Technological University (NTU), Singapore, in July 1998.

He is currently an Assistant Professor of Electrical and Computer Engineering at Utah State University, Logan, and the Acting Director of the Center for Self-Organizing and Intelligent Systems (CSOIS). His current research interests include robust iterative learning and repetitive control, identification and control of distributed parameter systems with networked movable actuators and sensors, autonomous ground mobile robots, fractional order dynamic systems and control, computational intelligence, intelligent mechatronic systems, and visual servoing/tracking. He holds 12 granted and two pending U.S. patents in various aspects of hard disk drive servomechanics. He published more than 150 papers in refereed journals and conferences and more than 50 industrial technical reports. He coauthored a research monograph *Iterative Learning Control: Convergence, Robustness and Applications* (with Changyun Wen, Lecture Notes Series in Control and Information Science, Springer-Verlag, Berlin, Germany, 1999) and two textbooks *System Simulation: Techniques and Applications Based on MATLAB/Simulink* (with Dingyü Xue, ISBN 7-302-05341-3/TP3137, Tsinghua University Press, Beijing, China, 2002) and *Solving Advanced Applied Mathematical Problems Using Matlab* (with Dingyü Xue, ISBN 7-302-09311-3/O.392, Tsinghua University Press, Aug. 2004).

Dr. Chen is an Associate Editor on the Conference Editorial Board of Control Systems Society of IEEE and an Associate Editor on the ISA Editorial Board for American Control Conference.

**Huifang Dou** (S'96–M'04) received the B.S. degree in electrical engineering from Wuhan University of Technology, Wuhan, China, in 1985, the M.S. degree in automatic control from Beijing Institute of Technology, Beijing, China, in 1988, and the Ph.D. degree in mechanism and precision instruments from Tsinghua University, Beijing, in 1997.

From 1997 to 2001, she was a Postdoctoral Fellow and Research Fellow with the Electrical and Computer Engineering Department as well as the Obstetrics and Gynecology Department at National University of Singapore, Singapore. She is currently a Research Assistant Professor in the Electrical and Computer Engineering Department and the Biological and Irrigation Engineering Department at Utah State University. Her research interests include biomechanics, precision motion control and modeling, smart sensors and actuators, instrumentation, and their applications to the biomedical and rehabilitation engineering.

Dr. Dou is a Member of the IEEE Engineering in Medicine and Biology Society.